Journal of Current Chemical & Pharmaceutical Sciences

J. Curr. Chem. Pharm. Sc.: 2(4), 2012, 316-333
ISSN 2277-2871

MOLECULAR DESCRIPTORS IN THE RATIONALE OF α- AND β- SULFONE PIPERIDINE HYDROXAMATE INHIBITORS OF TACE AND MMP

P. SINGH[*] and NIDHI SHEKHAWAT[a]

Department of Chemistry, S.K. Government College, SIKAR – 332001 (Raj.) INDIA
[a]Department of Zoology, Gramin Mahila P. G. College, SIKAR – 332001 (Raj.) INDIA

(*Received : 02.10.2012; Accepted : 11.10.2012*)

ABSTRACT

Tumor necrosis factor-α converting enzyme (TACE) and matrix metalloproteinases (MMP-2 and MMP-13) inhibition activities of α- and β-sulfone piperidine hydroxamic acid derivatives have been quantitatively analyzed in terms of chemometric descriptors. The identified descriptors, have highlighted the role of the weaker forces (polarization or van der Waals types) and the electronic effect for inhibition of the TACE. The flexibility in a compound and presence of certain structural fragments are prerequisite for inhibition of the MMP-2 while the atom centered fragments, in addition to some structural moieties are responsible for inhibition of the MMP-13. PLS analysis has further confirmed the dominance of the CP-MLR identified descriptors. Applicability domain analysis revealed that the suggested models have acceptable predictability. Except one outlier compound predicted for MMP-2 activity, all the compounds were within the applicability domain of the proposed models of TACE, MMP-13 and MMP-2 activities and were evaluated correctly. The guidelines provided may be helpful in exploring more potential analogues of the series.

The *in vivo* inhibition activities for LPS-stimulated TNF production in Raw Cells and human whole blood (HWB), reported for a few compounds, have also been correlated with such descriptors. The descriptors for inhibition of Raw Cells have emphasized the significance of lag 2 and lag 3 of autocorrelations weighted, respectively, by atomic van der Waals volumes and atomic Sanderson electronegativities. The electronic and polarizability weighted descriptors, on the other hand, have exhibited their importance in the inhibition of HWB.

Key words: TNF-α converting enzyme (TACE) inhibitors, MMP inhibitors, Combinatorial protocol in multiple linear regression (CP-MLR) analysis, Chemometric descriptors, Sulfone piperidine hydroxamic acid derivatives, QSAR.

INTRODUCTION

Tumor necrosis factor-α (TNF-α) is one of the cytokines, which is involved in immunomodulation and proinflammation events. The overproduction of TNF-α has been concerned in many autoimmune disorders namely rheumatoid arthritis, Crohn's disease and psoriasis[1-4]. The reduction of TNF-α level has been managed for successful treatment of inflammatory diseases[5]. Thus, the finding of a low cost, orally active small drug which could moderate TNF-α levels is of prime importance at clinical level at present. One important strategy to reduce the levels of soluble TNF-α is to block the release of TNF-α from the cell surface by the inhibition of TNF-α converting enzyme (TACE) [6-8]. This enzyme being a membrane-bound

Available online at www.sadgurupublications.com
[*]Author for correspondence; E-mail: psingh_sikar@rediffmail.com; Ph.: +91.1572.251039; Fax: +91.1572.270039

zinc-metalloprotease is able to convert the 26-kD transmembrane pro-form of TNF-α to the mature 17-kD soluble form[9,10]. It was shown that the active site of TACE shares many common features with the matrix metalloproteinases (MMP's) [11,12], therefore, depending on the scaffold used, different inhibitors can provide varying cellular activity and selectivity of TACE.

Previously, it was reported that butynyloxyphenyl moiety attached to α- and β-sulfone piperidine hydroxamate scaffolds can provide potent TACE inhibitors[13-15]. From these inhibitors, the β-sulfone piperdine hydroxamates are generally more potent than α-sulfone piperdine hydroxamates in both the TACE enzyme and cellular assays. Though these inhibitors exhibited reasonable enzyme and cellular activity but revealed moderate activity in human whole blood (HWB). Also, they demonstrated poor pharmacokinetic properties, making it difficult to achieve and sustain plasma levels above the HWB IC_{50} (concentration required to bring out 50% inhibition). To further improve activity and selectivity, the piperidine α-sulfone hydroxamate scaffold bearing butynyloxyl group constant has been optimized[14] so far in which the substituent on the piperidine nitrogen were only varied. Replacement of butynyloxyl group with quinolinylmethyl ether moiety has been shown to provide very active and extremely selective TACE inhibitors[15]. In view of this fact, the α-sulfone hydroxamate scaffold attached with quinolinylmethyl ether moiety has been recently explored[16]. However these studies were targeted at the alterations of substituents at piperidine nitrogen in a trial-and-error manner.

The present communication is, therefore, aimed at to perform a quantitative structure-activity relationship (QSAR) study on α- and β-sulfone piperidine hydroxamate derivatives so as to provide the rationale for drug-design and to explore the possible mechanism of action. In the congeneric series, where a relative study is being performed, the chemometric 2D-descriptors may play important role in deriving the significant relationships with biological activities of the compounds. The novelty and importance of a 2D-QSAR study is due to its simplicity for the calculations of different descriptors and their interpretation (in physical sense) to explain the biological activities of compounds at molecular level.

EXPERIMENTAL

Materials and methods

The compounds under investigation include α- and β-sulfone piperidine hydroxamate derivatives having substituent variations at piperidine nitrogen. These analogues along with their inhibition activity, IC_{50} values for TACE, MMP-2, MMP-13, Raw Cells and HWB, were taken from the literature[16] and the same, expressed as pIC_{50} ($-\log IC_{50}$) on molar basis, are listed in Table 1. A total number of 23 compounds, having general structures as in Figure 1, have been considered for present investigation.

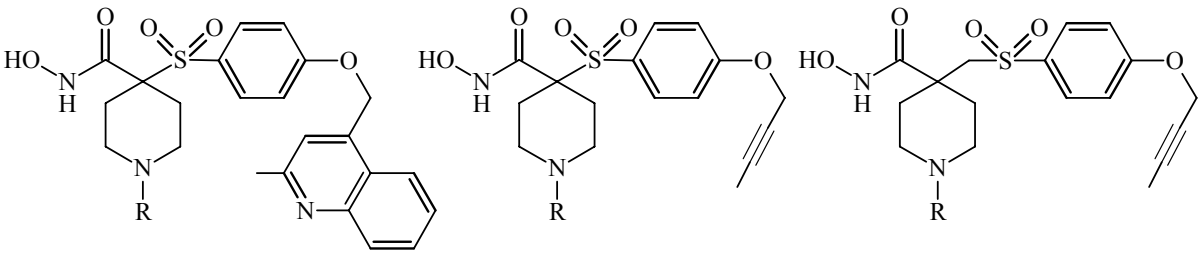

A (1-14) **B (15-19)** **C (20-23)**

Fig. 1: General structures of piperidine hydroxamic acid derivatives; (A) Quinolinylmethyl ether α-sulfones, (B) Butynyloxy α-sulfones and (C) Butynyloxy β-sulfones

Table 1: Observed and modeled inhibition activities of α- and β-sulfone piperidine hydroxamic acid derivatives (Figure 1 for structures)

Compd.	R	pIC_{50} (M)											
		TACE			MMP-13			MMP-2			Raw Cells		HWB	
		Obsd.[a]	Calcd.		Obsd.[a]	Calcd.		Obsd.[a]	Calcd.		Obsd.[a]	Calcd.	Obsd.[a]	Calcd.
			Eq. (3)	PLS		Eq. (6)	PLS		Eq. (9)	PLS		Eq. (13)		Eq. (14)
A1[b]	H	7.481	7.933	7.882	5.064	5.467	5.540	< 4.824[c]	5.703	5.709	6.476	6.602	5.620	5.606
A2	CHO	8.699	8.450	8.326	6.357	6.502	6.310	5.854	5.703	5.721	7.167	6.955	5.886	6.090
A3[b]	Ac	9.000	8.579	8.567	5.874	6.428	6.611	5.158	5.703	5.727	6.415	6.510	5.824	5.907
A4	COiPr	8.699	8.413	8.625	6.382	6.279	6.521	5.906	5.703	5.908	< 6.000[c]	6.576	4.854	4.744
A5	COPh	9.000	8.497	8.754	6.690	6.353	6.624	6.287	6.261	6.212	< 6.000[c]	5.595	4.553	4.751
A6	CO-4-Py	8.699	8.756	8.760	6.457	6.390	6.505	5.961	6.261	6.154	6.638	6.546	5.721	5.334
A7	Boc	> 9.000[c]	8.501	8.370	5.955	6.204	6.119	5.573	5.703	5.639	< 6.000[c]	6.757	< 4.301[c]	4.873
A8	CONHEt	8.699	8.598	8.758	6.078	5.821	5.965	5.442[d]	6.375	6.417	6.620	6.644	5.602	5.565
A9	$CONEt_2$	8.523	8.473	8.698	7.244	7.248	7.214	7.018	7.047	6.869	< 6.000[c]	6.946	< 4.301[c]	4.629
A10[b]	Me	7.959	7.446	7.680	5.838	6.428	6.360	4.821	5.703	5.475	6.903	6.981	5.620	5.517
A11	CH_2-4-Py	8.046	8.496	8.243	6.575	6.856	6.740	6.068	6.375	6.399	6.423	6.586	4.959	4.988
A12[b]	CH_2Ph-3,4-Cl	7.187	7.616	8.188	7.097	6.893	6.779	6.839	6.375	6.694	< 6.000[c]	6.537	< 4.301[c]	5.453
A13	SO_2Me	8.921	8.812	8.834	6.406	6.428	6.211	5.759	5.703	5.657	6.462	6.367	5.553	5.558
A14	SO_2iPr	8.000	8.304	8.357	6.033	6.279	5.980	5.670	5.703	5.582	< 6.000[c]	6.384	4.854	5.090
B15	H	6.697	6.725	6.522	5.396	5.653	5.584	NR	--	--	NR	--	NR	--
B16	Ac	7.328	7.485	7.258	6.866	6.614	6.705	NR	--	--	NR	--	NR	--
B17[b]	COPh	7.137	7.494	7.526	6.979	6.539	6.710	NR	--	--	NR	--	NR	--
B18	Boc	6.873	7.123	6.995	6.547	6.390	6.469	NR	--	--	NR	--	NR	--
B19	CH_2Ph-3,4-Cl	6.827	6.634	6.965	7.143	7.080	6.858	NR	--	--	NR	--	NR	--
C20[b]	H	9.000	8.706	8.380	5.721	6.119	6.041	5.799	6.375	6.603	NR	--	NR	--
C21	Ac	8.699	9.156	8.850	6.810	7.080	7.155	6.467	6.375	6.594	6.310	6.287	5.060	5.071
C22	COPh	9.000	8.878	8.959	7.229	7.005	7.166	7.208	6.933	7.037	6.398	6.362	5.602	5.345
C23	Boc	8.699	8.607	8.504	6.870	6.856	6.910	NR	--	--	6.208	6.179	4.854	4.996

[a]The IC_{50} values were taken from ref. (16). [b]Test set compound. [c]Eliminated compound from the study due to uncertain inhibition activity.
[d]"Outlier" compound. NR; activity is not reported

For modeling purpose, the data sets, related to TACE, MMP-2 and MMP-13 inhibition activities, were divided into training and test sets to insure external validation of models derived from appropriate descriptors. Additionally, the leave-one-out (LOO) and leave-five-out (L5O) procedures were employed for internal validation of such models. The selection of compounds for test set has been made through SYSTAT[17] using the single linkage hierarchical cluster procedure involving the Euclidean distances of the activity, pIC_{50}, values. Nearly 25% of the compounds, from total population, were selected from the generated cluster tree in such a way to keep them at a maximum possible distance from each other. In SYSTAT, by default, the normalized Euclidean distances are computed to join the objects of cluster. The normalized distances are root mean-squared distances. The single linkage uses distance between two closest members in clustering. It generates long clusters and provides scope to choose objects at different intervals. Due to this reason, a single linkage clustering procedure was applied. However, the criterion of test set was improper for the inhibition of Raw Cells and the HWB due to limited activity data reported for them.

Molecular descriptors

The structures of the compounds under study have been drawn in 2D ChemDraw[18] using the standard procedure. All these structures have been ported to DRAGON software[19] for computing the descriptors corresponding to 0D-, 1D-, and 2D-classes. Table 2 provides the definition and scope of these descriptor-classes in addressing the structural features which were employed in the present work. The combinatorial protocol in multiple linear regression (CP-MLR) computational procedure[20] has been used in developing QSAR models. The descriptors of database have been scaled[21] so that their values remain between 0 and 1. The scaled descriptors would then show equal influence in the QSAR models and none dominate each other like in the case of pre-scaled descriptors with larger or smaller values.

Model development

The CP-MLR is a 'filter'-based variable selection procedure for model development in QSAR studies[20]. Its procedural aspects and implementation are discussed in some of our recent publications.[22-26] The developed software for this method has four embedded filters which make the variable selection process efficient and leads to a unique solution. Filter-1 seeds only those variables which have inter-parameter correlations to a predefined level (upper limit ≤ 0.79); filter-2 controls the variables entry to a regression equation through t-values of coefficients (threshold value ≥ 2.0); filter-3 provides comparability of equations with different number of variables in terms of square root of adjusted multiple correlation coefficient of regression equation, r-bar; filter-4 estimates the consistency of the equation in terms of cross-validated Q^2 with leave-one-out (LOO) cross-validation as default option (threshold value $0.3 \leq Q^2 \leq 1.0$). In order to collect the descriptors with higher information content and explanatory power, the threshold of filter-3 was successively incremented with increasing number of descriptors (per equation) by considering the r-bar value of the preceding optimum model as the new threshold for next generation.

To discover any chance correlations associated with the models obtained through CP-MLR, each cross-validated model has been put to a randomization test[27,28] by repeated randomization of the activity to ascertain the chance correlations, if any, associated with them. For this, every model has been subjected to 100 simulation runs with scrambled activity. The scrambled activity models with regression statistics better than or equal to that of the original activity model have been counted, to express the percent chance correlation of the model under scrutiny. Goodness of fit of models was assessed by examining the multiple correlation coefficient (r), the standard deviation (s), the F-ratio between the variances of calculated and observed activities (F).

The internal validation was ascertained through the cross-validated index, Q^2, from leave-one-out (Q^2_{LOO}) and leave-five-out (Q^2_{L5O}) procedures. A value greater than 0.5 of Q^2-index hints towards a

reasonable robust model. The external validation or predictive power of derived model is based on test set compounds. The statistical index r^2_{Test}, representing the squared correlation coefficient between the observed and predicted data of the test-set, has also been computed for this purpose. A value greater than 0.5 of r^2_{Test} suggests that the model obtained from training set has a reliable predictive power.

Table 2: Descriptor classes used for the analysis of inhibition activities of α- and β-sulfone piperidine hydroxamic acids

Descriptor class (acronyms)	Definition and scope
Constitutional (CONST)	Dimensionless or 0D descriptors; independent from molecular connectivity and conformations.
Topological (TOPO)	2D-descriptor from molecular graphs and independent conformations.
Molecular walk counts (MWC)	2D-descriptors representing self-returning walk counts of different lengths.
Modified Burden eigenvalues (BCUT)	2D-descriptors representing positive and negative eigenvalues of the adjacency matrix, weights the diagonal elements and atoms.
Galvez topological charge indices (GLVZ)	2D-descriptors representing the first 10 eigenvalues of corrected adjacency matrix.
2D-autocorrelations (2DAUTO)	Molecular descriptors calculated from the molecular graphs by summing the products of atom weights of the terminal atoms of all the paths of the considered path length (the lag).
Functional groups (FUNC)	Molecular descriptors based on the counting of the chemical functional groups.
Atom-centred fragments (ACF)	Molecular descriptors based on the counting of 120 atom-centred fragments, as defined by Ghose-Crippen.
Empirical (EMP)	1D-descriptors represent the counts of non-single bonds, hydrophilic groups and ratio of the number of aromatic bonds and total bonds in an H-depleted molecule.
Properties (PROP)	1D-descriptors representing molecular properties of a molecule.

Partial least squares analysis

Partial Least Squares[29-31] (PLS) linear regression is a method suitable for overcoming the problems in MLR related to multicollinear or over-abundant descriptors. This is a modeling technique where information in the descriptor matrix X is projected onto a small number of latent variables (LV) called PLS components, which are linear combination of the original variables. The matrix Y is simultaneously used in estimating the "latent" variables in X that will be most relevant to predict the Y variables. All descriptor variables are preprocessed by autoscaling, using weights based on the variables' standard deviation and the data are mean-centered prior to PLS processing. Scaling of descriptors is necessary because the values have different orders of magnitude.

Cross-validation was employed to select the used optimum number of LVs. With cross-validation, some samples were kept out of the calibration and used for prediction. The process was repeated so that each of the samples was kept out once. The predicted values of left-out samples were then compared to the observed values using predicted residual sum of squares (PRESS). The PRESS obtained in the cross-validation was calculated each time that a new LV was added to the model.

Applicability domain

The utility of a QSAR model is based on its accurate prediction ability for new compounds. A model is valid only within its training domain and new compounds must be assessed as belonging to the domain before the model is applied. The applicability domain is assessed by the leverage values for each compound[32,33]. The Williams plot (the plot of standardized residuals versus leverage values, h) can then be used for an immediate and simple graphical detection of both the response outliers (Y outliers) and structurally influential chemicals (X outliers) in the model. In this plot, the applicability domain is established inside a squared area within ± x× (s.d.) and a leverage threshold h^*. The threshold h^* is generally fixed at 3 (k + 1)/n (n is the number of training set compounds and k is the number of model parameters) whereas x = 2 to 3. Prediction must be considered unreliable for compounds with a high leverage value ($h > h^*$). On the other hand, when the leverage value of a compound is lower than the threshold value, the probability of accordance between predicted and observed values is as high as that for the training set compounds.

RESULTS AND DISCUSSION

A total number of 465 descriptors, belonging to 0D-2D classes of DRAGON, have been computed for 23 compounds of Table 1. Next, these descriptors have been scaled between 0 and 1 and collated in the separate pools, pertaining to inhibition activities of TACE, MMP-13, MMP-2, Raw Cells and HWB, for CP-MLR analyses. A test set has been selected through SYSTAT and the same was used for external validation of the models, derived from the training set compounds. Six compounds (**A1**, **A3**, **A10**, **A12**, **B17** and **C20**; Table 1) were identified for the test set for TACE, MMP-13 and MMP-2 activities while remaining compounds constitute the training set. A common test set was considered here to reveal the influence of similar structural features on these inhibition activities. Compounds having uncertain activity values have been eliminated from the data set prior to CP-MLR analysis. A number of models in one- two- and three-descriptors have been derived in succession. In doing so, filter-3 was in turn incremented with increasing number of descriptors (per equation) by considering the r-bar value of the preceding optimum model as the new threshold for next generation.

In order to quantify the TACE, MMP-13 and MMP-2 inhibition activity in terms of molecular descriptors, the corresponding training sets were employed to explore predictive models through CP-MLR. A total number of 17 and 8 models in three descriptors, respectively, for the TACE and MMP-13 activities and 8 models in two descriptors for the MMP-2 activity have divulged statistical significant parameters. However, three highest significant models for each of the TACE, MMP-13 and MMP-12 inhibition activities, are given by Equations (1)-(9)

$$pIC_{50}\ (TACE) = 8.596 - 5.256\ (0.821)\ SEigp - 1.882\ (0.297)\ JGI2 + 1.824\ (0.306)\ MATS6v$$

$$n = 16,\ r = 0.945,\ s = 0.302,\ F\ (3, 12) = 33.071,\ Q^2_{LOO} = 0.798,\ Q^2_{L5O} = 0.828,\ r^2_{Test} = 0.709 \quad \ldots(1)$$

$$pIC_{50}\ (TACE) = 8.451 - 5.771\ (0.820)\ SEigp - 1.680\ (0.293)\ JGI2 + 2.039\ (0.342)\ MATS6p$$

$$n = 16,\ r = 0.945,\ s = 0.302,\ F\ (3, 12) = 33.098,\ Q^2_{LOO} = 0.785,\ Q^2_{L5O} = 0.823,\ r^2_{Test} = 0.645 \quad \ldots(2)$$

$$pIC_{50}\ (TACE) = 10.560 - 6.029\ (0.818)\ SEigp - 1.834\ (0.293)\ JGI2 - 1.973\ (0.328)\ GATS6v$$

$$n = 16,\ r = 0.945,\ s = 0.300,\ F\ (3, 12) = 33.595,\ Q^2_{LOO} = 0.793,\ Q^2_{L5O} = 0.767,\ r^2_{Test} = 0.742 \quad \ldots(3)$$

$$pIC_{50}\ (MMP\text{-}13) = 6.561 + 1.050\ (0.194)\ nCs - 0.990\ (0.181)\ H\text{-}050 - 0.422\ (0.197)\ H\text{-}052$$

n = 17, r = 0.901, s = 0.236, F (3, 13) = 18.657, Q^2_{LOO} = 0.653, Q^2_{L5O} = 0.619, r^2_{Test} = 0.728 …(4)

pIC_{50} (MMP-13) = 6.283 + 1.033 (0.189) nCs + 0.284 (0.124) C-040 – 0.804 (0.181) H-050

n = 17, r = 0.905, s = 0.232, F (3, 13) = 19.515, Q^2_{LOO} = 0.719, Q^2_{L5O} = 0.619, r^2_{Test} = 0.721 …(5)

pIC_{50} (MMP-13) = 6.688 – 0.521 (0.228) nH + 1.081 (0.193) nCs – 1.035 (0.182) H-050

n = 17, r = 0.905, s = 0.232, F (3, 13) = 19.533, Q^2_{LOO} = 0.536, Q^2_{L5O} = 0.627, r^2_{Test} = 0.715 …(6)

pIC_{50} (MMP-2) = 5.526 + 0.850 (0.356) VEA1 + 1.140 (0.256) nCs

n = 11, r = 0.891, s = 0.274, F (2, 8) = 15.355, Q^2_{LOO} = 0.512, Q^2_{L5O} = 0.568, r^2_{Test} = 0.738 …(7)

pIC_{50} (MMP-2) = 6.265 + 1.213 (0.273) PHI – 1.585 (0.287) C-011

n = 11, r = 0.917, s = 0.240, F (2, 8) = 21.074, Q^2_{LOO} = 0.643, Q^2_{L5O} = 0.672, r^2_{Test} = 0.639 …(8)

pIC_{50} (MMP-2) = 5.703 + 1.344 (0.195) nCs + 0.558 (0.144) nCONR2Ph

n = 11, r = 0.937, s = 0.211, F (2, 8) = 28.638, Q^2_{LOO} = 0.746, Q^2_{L5O} = 0.756, r^2_{Test} = 0.522 …(9)

In all emerged models, the F-values remained significant at 99% level [$F_{2,8}$ (0.01) = 8.649, $F_{3,12}$ (0.01) = 5.953 and $F_{3,13}$ (0.01) = 5.739] and the standard errors of regression coefficients (data within the parentheses) were significant at more than 95% level. The indices Q^2_{LOO} and Q^2_{L5O} (> 0.5) have accounted for internal robustness of the developed models while the index r^2_{Test} greater than 0.5 specified that the selected test set is accountable for external validation of these models. The signs of the regression coefficients have indicated the direction of influence of explanatory variables; the positive regression coefficient associated to a descriptor will augment the activity profile of a compound while the negative coefficient will cause detrimental effect to it. In fact, 17, 8 and 8 models developed, respectively, for the inhibition of TACE, MMP-13 and MMP-2, in the same order, have 20, 11 and 12 shared descriptors among individual activity profile. The shared descriptors along with their class, brief description, average regression coefficients and total incidences are given in Table 3. The participated descriptors, in the listed Equations (1)-(9), are the highly influential ones to address the biological effects of compounds.

In Equations (1)-(3) the descriptors, SEigp and JGI2 representing, respectively the eigenvalue sum from polarizability weighted distance matrix and the mean topological charge index of order 2, are the common variables of Equations (1)-(3) and remained the negative contributors to activity. The descriptors, GATS6v, and MATS6p and MATS6v characterizing the autocorrelations of Geary and Moran, respectively, and displayed the importance of lag (path) 6 which is weighted either by atomic van der Waals volumes (v) or atomic polarizabilities (p). The GATS6v has negative impact on TACE inhibition activity (Equation 3) while MATS6p (Equation 2) or MATS6v (Equation 1) has positive effect on it. From participating descriptors of Equations (1)-(3), it appeared that the weaker forces (polarization or van der Waals types) and the electronic effect dominate for inhibition of the TACE.

In Equations (4)-(6) the descriptors, nCs and C-040 accounting, respectively, for the number of total secondary carbons (sp^3) and the fragments such as R-C(=X)-X/ R-C#X/ X=C=X have made positive influence on activity. The atom centered fragment descriptors nH, H-050 and H-052 are the representative of number of hydrogen atoms, hydrogen attached to heteroatom and hydrogen attached to C0(sp^3) with one X attached to next C respectively. The latter three descriptors, on the other hand, have imparted negative effect on MMP-13 inhibition activity. Thus, these atom centered fragments or the structural moieties are responsible for inhibition of the MMP-13.

Table 3: Identified descriptors[a] along with their physical meaning, average regression coefficient and incidence[b], in modeling of TACE, MMP-13 and MMP-2 inhibition activities

S. No.	Name	Class	Physical meaning	TACE	MMP-13	MMP-2
1	nH	CONST	Number of Hydrogen atoms		-0.521 (1)	
2	D/Dr10	TOPO	Distance/detour ring index of order 10		-0.255 (1)	
3	PHI	TOPO	Kier flexibility index			1.258 (3)
4	PW5	TOPO	Path/walk 5 – Randic shape index	0.802 (1)		
5	S2K	TOPO	2-Path Kier alpha-modified shape inded			0.782 (1)
6	SEigp	TOPO	Eigenvalue sum from polarizability weighted distance matrix	-5.435 (9)		
7	SEigv	TOPO	Eigenvalue sum from van der Waals weighted distance matrix	-5.744 (4)		
8	SPI	TOPO	Superpendentic index		-0.591(1)	
9	T(N..O)	TOPO	Sum of topological distances between N..O		-0.337 (1)	
10	T(N..S)	TOPO	Sum of topological distances between N..S		-0.370 (1)	
11	TI2	TOPO	Second Mohar index	1.948 (2)		
12	TIE	TOPO	E-state topological parameter	-0.890 (2)		
13	VAR	TOPO	Variation index			0.645 (2)
14	VEA1	TOPO	Eigenvector coefficient sum from adjacency matrix			0.850 (1)
15	X1A	TOPO	Average connectivity index chi-1			1.320 (1)
16	X3A	TOPO	Average connectivity index chi-3			1.285 (1)
17	GGI4	GLVZ	Topological charge index of order 4	2.398 (1)		
18	GGI5	GLVZ	Topological charge index of order 5	2.130 (1)		
19	JGI2	GLVZ	Mean topological charge index of order 2	-1.858 (7)		
20	ATS3e	2DAUTO	Broto-Moreau autocorrelation of a topological structure – lag 3/ weighted by atomic Sanderson electronegativities		-0.419 (1)	

Cont…

S. No.	Name	Class	Physical meaning	TACE	MMP-13	MMP-2
21	GATS2p	2DAUTO	Geary autocorrelation – lag 2/ weighted by atomic polarizabilities	2.339 (3)		
22	GATS3p	2DAUTO	Geary autocorrelation – lag 3/ weighted by atomic polarizabilities	-1.732 (5)		
23	GATS4v	2DAUTO	Geary autocorrelation – lag 4/ weighted by atomic van der Waals volumes			1.292 (1)
24	GATS6p	2DAUTO	Geary autocorrelation – lag 6/ weighted by atomic polarizabilities	-2.040 (1)		
25	GAT S6v	2DAUTO	Geary autocorrelation – lag 6/ weighted by atomic van der Waals volumes	-1.667 (3)		
26	GATS8v	2DAUTO	Geary autocorrelation – lag 8/ weighted by atomic van der Waals volumes	1.111 (2)		
27	MATS2p	2DAUTO	Moran autocorrelation – lag 2/ weighted by atomic polarizabilities	-1.550 (1)		
28	MATS2v	2DAUTO	Moran autocorrelation – lag 2/ weighted by atomic van der Waals volumes			
29	MATS3m	2DAUTO	Moran autocorrelation – lag 3/ weighted by atomic masses			
30	MATS3p	2DAUTO	Moran autocorrelation – lag 3/ weighted by atomic polarizabilities			1.895 (1)
31	MATS4p	2DAUTO	Moran autocorrelation – lag 4/ weighted by atomic polarizabilities		-0.556 (1)	
32	MATS4v	2DAUTO	Moran autocorrelation – lag 4/ weighted by atomic van der Waals volumes			-1.484 (1)
33	MATS6p	2DAUTO	Moran autocorrelation – lag 6/ weighted by atomic polarizabilities	2.037 (2)		
34	MATS6v	2DAUTO	Moran autocorrelation – lag 6/ weighted by atomic van der Waals volumes	1.539 (3)		
35	MATS8v	2DAUTO	Moran autocorrelation – lag 8/ weighted by atomic van der Waals volumes	-1.158 (1)		
36	nCONR2	FUNC	Number of tertiary amides (aliphatic)	0.458 (1)		
37	nCONR2Ph	FUNC	Number of tertiary amides (aromatic)			0.558 (1)
38	nCs	FUNC	Number of total secondary carbons (sp^3)		0.966 (9)	1.242 (2)
39	C-011	ACF	Fragment corresponds to CR3X	-2.472 (1)		-1.585 (1)
40	C-040	ACF	R-C(=X)-X/ R-C#X/ X=C=X		0.284 (1)	
41	H-050	ACF	Hydrogen attached to heteroatom		-0.964 (9)	
42	H-052	ACF	Hydrogen attached to C0(sp^3) with one X attached to next C		-0.422 (1)	
43	N-072	ACF	Fragment corresponds to RCO-N< / >N-X=X	0.547 (1)		

[a]The descriptors have been identified from the models, emerged from CP-MLR protocol with a training set of 16, 17 and 11 compounds for TACE, MMP-13 and MMP-2 inhibition activities respectively. [b]The average regression coefficient of the descriptor corresponding to all models and the total number of its incidence. The arithmetic sign of the coefficient represents the actual sign of the regression coefficient in the models.

In Equations (7)-(9) the descriptors, PHI, VEA1, nCs and nCONR2Ph denoting, respectively, the Kier flexibility index, the eigenvector coefficient sum from adjacency matrix, number of total secondary carbons (sp^3) and number of tertiary amides (aromatic). These descriptors have shown incremental effect on MMP-2 inhibition activity while the descriptor, C-011, corresponds to the fragment CR3X, has detrimental effect on it. One compound (**A8**; Table 1) remained outlier and the same was eliminated from the data set while deriving models for MMP-2 activity. Possibly, the compound entails an error in the determination of its inhibition activity. From developed models, it appeared that the flexibility and presence of certain structural fragment in a compound are prerequisite for inhibition of the MMP-2.

Equations (3), (6) and (9), being the most significant models, have been retained for further discussion. The calculated inhibition activities, using these equations, for TACE, MMP-13 and MMP-2 have been documented in Table 1. The same remained in parity with the observed ones. The variations between observed and calculated pIC_{50} values for TACE, MMP-13 and MMP-2 activities, displaying the training set and test set compounds, are given in Figure 2. For each activity the compounds have exhibited the systematic variations, reflecting upon the goodness of fit of these models.

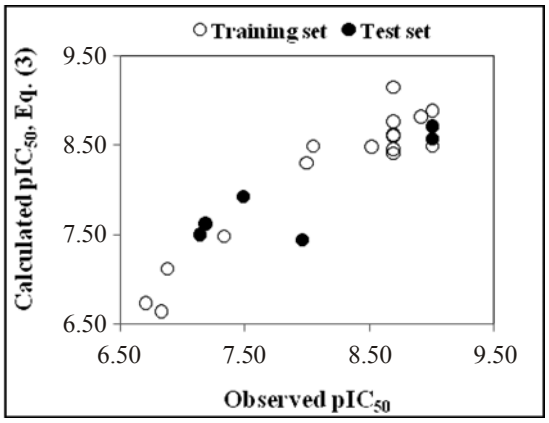

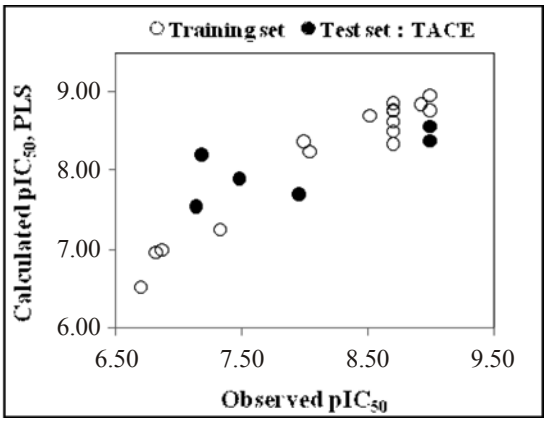

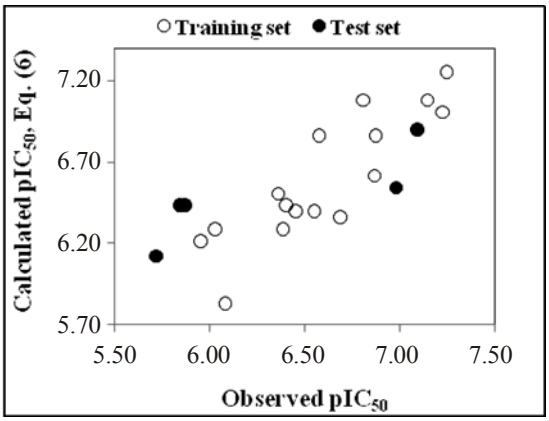

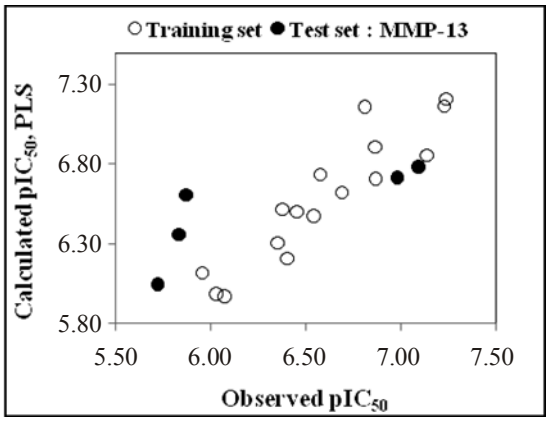

Cont…

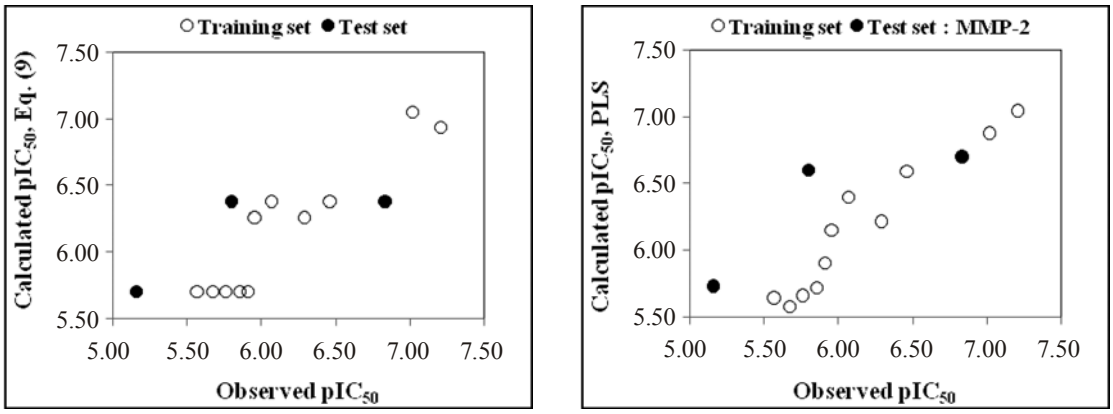

Fig. 2: Plot of observed versus caculated pIC_{50} values relating to inhibition of TACE, MMP-13 and MMP-2 for training set and test set compounds

From Equation (3), it appeared that the lower values of descriptors SEigp, JGI2 and GATS6v are beneficial in improving the TACE inhibition activity of a compound. Similarly, Equation (6) and (9) may be used to further improve the MMP-13 and MMP-2 activities of a compound. The presence of higher number of aromatic tertiary amides in addition to higher number of total secondary carbons (sp^3) and lower number of hydrogen atom or lower number of hydrogen attached to heteroatom are the essential features of a compound to make it an effective inhibitor of MMP-13 and MMP-2.

Further, the PLS analyses have also been performed on 20, 11 and 12 identified descriptors related, respectively, to TACE, MMP-13 and MMP-2 inhibition activities of the compounds and the results are summarized in Table 4. In the study, the descriptors were autoscaled (zero mean and unit standard deviation) to provide each one of them equal weightage. In the PLS cross-validation, two-components remained optimum for each of these 20, 11 and 12 descriptors and they have explained, respectively, 94.7%, 89.3% and 88.2% of variances in the said activities. The PLS equations of optimum two-components and MLR-like PLS coefficients of identified descriptors for TACE, MMP-13 and MMP-2 activities are given in Table 4. The calculated activity values of training and test set compounds remained in close agreement to that of the observed ones and are listed in Table 1. For comparison, the plot between observed and calculated activities (through PLS analyses) for the training and test set compounds is given in Figure 2. Figure 3 shows a plot of the fraction contribution of normalized regression coefficients of these descriptors to the activity (Table 4). Different orders, indicating the level of significance, of 20, 11 and 12 descriptors, respectively, for TACE, MMP-13 and MMP-2 activities are included in Table 4. For a given descriptor, lower is the order higher would be its significance in addressing the biological activity.

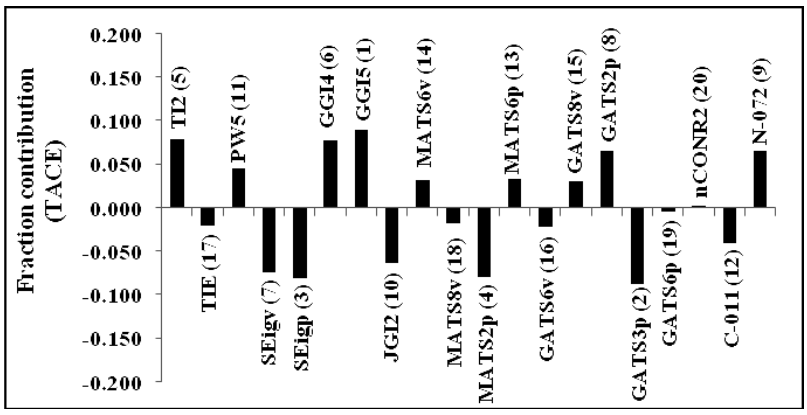

Cont…

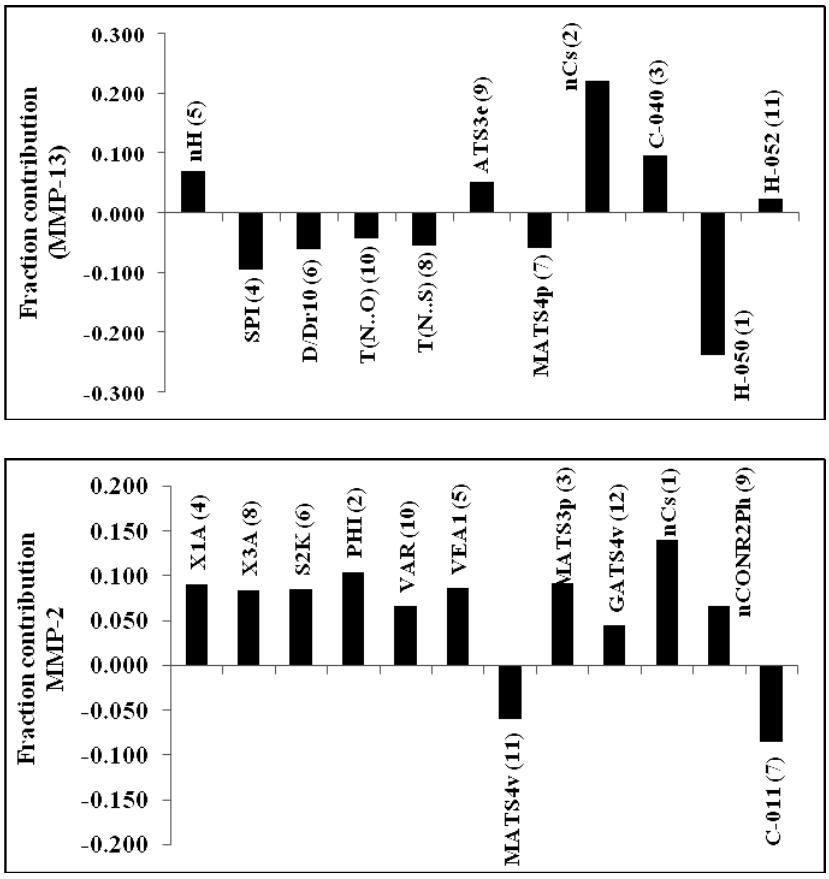

Fig. 3: Plot of fraction contribution of MLR-like PLS coefficients (normalized) against 20, 11 and 12 identified descriptors (Table 4) associated, resepectively, with TACE, MMP-13 and MMP-2 inhibition activities of the compounds

Table 4: PLS and MLR-like PLS models from the descriptors of three parameter CP-MLR models for TACE, MMP-13 and MMP-2 inhibition activities

A: PLS equation				B: PLS regression statistics			
PLS components	PLS coefficient (s.e.)[a]			Symbol	Estimate		
	TACE	MMP-13	MMP-2		TACE	MMP-13	MMP-2
Component-1	0.300 (0.021)	-0.247 (0.026)	-0.221 (0.029)	n	16	17	11
Component-2	-0.108 (0.024)	-0.113 (0.022)	-0.061 (0.034)	r	0.973	0.945	0.939
Constant	8.213	6.532	6.161	s	0.206	0.171	0.207
				F	113.344	58.655	29.643
				Q^2_{LOO}	0.916	0.800	0.654
				Q^2_{L5O}	0.917	0.784	0.579
				r^2_{Test}	0.515	0.689	0.656

C: MLR-like PLS Equation

S. No.	TACE			MMP-13			MMP-2		
	Descriptor	**MLR-like coefficient (f. c.)[b]**	**Order**	**Descriptor**	**MLR-like coefficient (f. c.)[b]**	**Order**	**Descriptor**	**MLR-like coefficient (f. c.)[b]**	**Order**
1	TI2	0.334 (0.079)	5	nH	0.280 (0.070)	5	X1A	0.229 (0.090)	4
2	TIE	-0.096 (-0.020)	17	SPI	-0.344 (-0.094)	4	X3A	0.202 (0.084)	8
3	PW5	0.192 (0.045)	11	D/Dr10	-0.136 (-0.059)	6	S2K	0.206 (0.085)	6
4	SEigv	-1.138 (-0.073)	7	T(N..O)	-0.129 (-0.042)	10	PHI	0.301 (0.104)	2
5	SEigp	-1.157 (-0.080)	3	T(N..S)	-0.175 (-0.053)	8	VAR	0.138 (0.066	10
6	GGI4	0.425 (0.077)	6	ATS3e	0.184 (0.051)	9	VEA1	0.286 (0.086)	5
7	GGI5	0.532 (0.089)	1	MATS4p	-0.285 (-0.057)	7	MATS4v	-0.178 (-0.058)	11
8	JGI2	-0.324 (-0.063)	10	nCs	0.777 (0.220)	2	MATS3p	0.338 (0.091)	3
9	MATS6v	0.169 (0.031)	14	C-040	0.212 (0.095)	3	GATS4v	0.128 (0.045)	12
10	MATS8v	-0.101 (-0.018)	18	H-050	-0.786 (-0.236)	1	nCs	0.334 (0.140)	1
11	MATS2p	-0.417 (-0.079)	4	H-052	0.082 (0.023)	11	nCONR2Ph	0.117 (0.067)	9
12	MATS6p	0.197 (0.032)	13	Constant	6.436		C-011	-0.257 (-0.084)	7
13	GATS6v	-0.124 (-0.021)	16				Constant	5.500	
14	GATS8v	0.167 (0.030)	15						
15	GATS2p	0.430 (0.065)	8						
16	GATS3p	-0.434 (-0.087)	2						
17	GATS6p	-0.022 (-0.004)	19						
18	nCONR2	0.008 (0.002)	20						
19	C-011	-0.252 (-0.040)	12						
20	N-072	0.276 (0.064)	9						
	Constant	7.770							

[a]Regression coefficient of PLS factor and its standard error. [b]Coefficients of MLR-like PLS equation in terms of descriptors for their original values; f.c. is fraction contribution of regression coefficient, computed from the normalized regression coefficients obtained from the autoscaled (zero mean and unit standard deviation) data

The descriptors having positive contribution will augment the activity and their higher values are desirable to further improve it. On the other hand, the descriptors having negative contribution will diminish the activity. The lower or more negative values of such descriptors may, therefore, enhance the activity of a compound.

The applicability domain (AD) has been analyzed for the models based on whole data-set relating to the TACE, MMP-13 and MMP-2 inhibition activities. It is characterized by the Williams plot of standardized residuals versus leverage (h_i) values. For this purpose, the participated descriptors in the most significant Equations (3), (6) and (9) have been considered to derive corresponding models based on whole data sets. The developed models are given in Equations (10)-(12) while standardized residuals and leverage values, calculated in conjunction with them, are further used to ascertain their ADs.

pIC_{50} (TACE) = 10.673 –6.270 (0.794) SEigp –1.862 (0.298) JGI2 – 2.167 (0.337) GATS6v

n = 22, r = 0.923, s = 0.340, F (3, 18) = 34.646, Q^2_{LOO} = 0.788, Q^2_{L5O} = 0.770 …(10)

pIC_{50} (MMP-13) = 6.656 –0.555 (0.279) nH + 1.197 (0.226) nCs – 1.122 (0.181) H-050

n = 23, r = 0.883, s = 0.300, F (3, 19) = 22.525, Q^2_{LOO} = 0.676, Q^2_{L5O} = 0.634 …(11)

pIC_{50} = 5.517 + 1.576 (0.317) nCs + 0.706 (0.245) nCONR2Ph

n = 15, r = 0.847, s = 0.377, F (2, 12) = 15.178, Q^2_{LOO} = 0.602, Q^2_{L5O} = 0.643 …(12)

The limits of normal values for the standardized residuals (response or Y outliers) were set as ±2×(s.d.) while leverage threshold as h* [= 3(k+1)/n; k is number of independent descriptors and n is number of compounds used in the derivation of model]. The graphical representations for the models related to the TACE, MMP-13 and MMP-2 inhibition activities, delineating the training set and the test set compounds is given in Figure 4. For both the training and test set compounds, the suggested models match the high quality parameters with good fitting power and the capability of assessing external data. Further, all of the compounds were within the AD of TACE and MMP-13 models. However, except one obvious "outlier" (compound **A8**; Table 1), all other compounds also remained within the AD of MMP-2 model. This connotes that the models under consideration are able to evaluate, both the training and test set compounds, correctly.

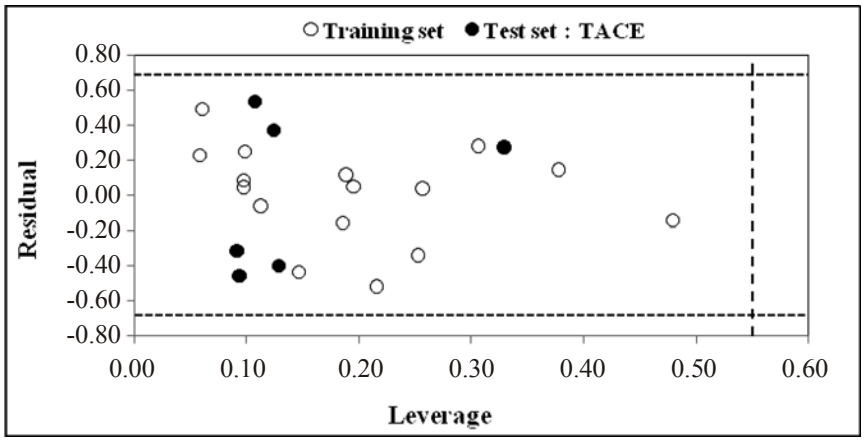

Cont…

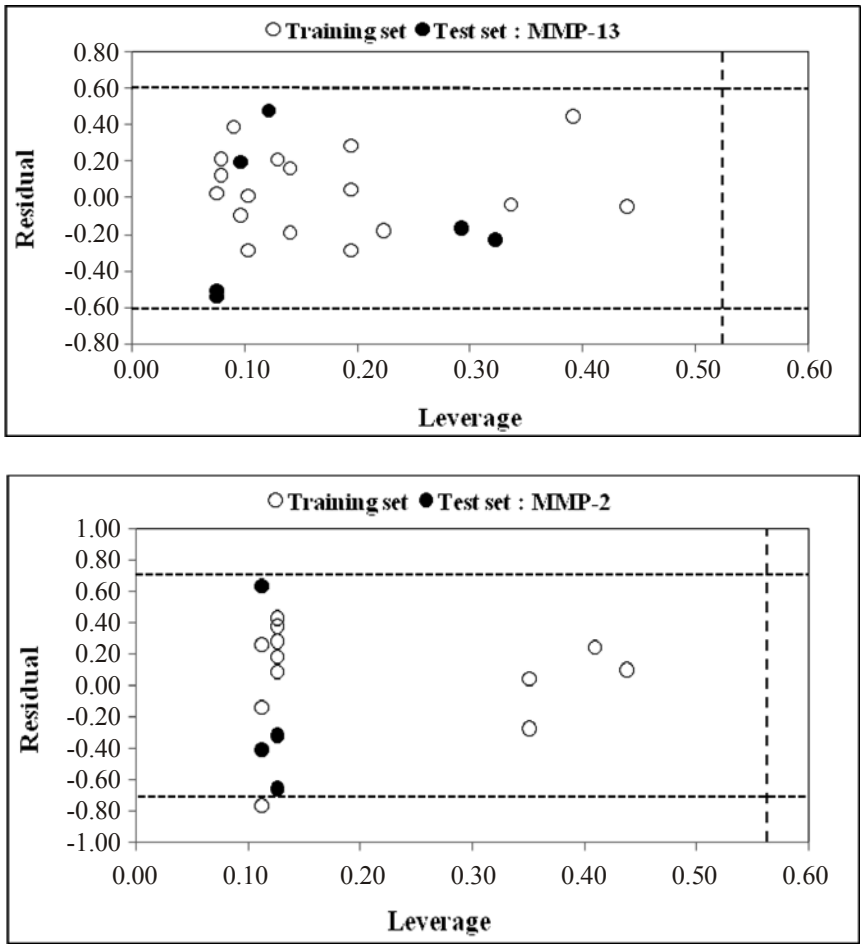

Fig. 4: Williams plot for whole data-set for TACE, MMP-13 and MMP-2 inhibition activities of α- and β-sulfone piperidine hydroxamic acid derivatives, listed in Table 1 (h* values, in that order, are 0.545, 0.522 and 0.563 and residual limits are ± 2.0 × s.d.)

A few α- and β-sulfone piperidine hydroxamates have also been evaluated for their ability to inhibit LPS-stimulated TNF production in Raw cells and in human whole blood (HWB). The *in vivo* inhibition activities (pIC_{50}) for these compounds have been included in Table 1. However the activity data, after eliminating uncertain values, remained insufficient to consider a test set for external validation. Therefore, models have been developed from whole data set for these two activities. For this, the computed and scaled 465 chemometric descriptors were subjected to CP-MLR to derive models for 11 and 14 compounds active towards Raw Cells and HWB respectively. A total number of 6 models in two descriptors for Raw Cell and 38 models in three descriptors for HWB were obtained and the highest significant of them for individual activity are given in Equation (13) and (14).

pIC_{50} (Raw Cells) = 6.533 + 0.616 (0.153) MATS2v – 0.820 (0.141) GATS3e

n = 11, r = 0.916, s = 0.124, F (2, 8) = 20.755, Q^2_{LOO} = 0.686, Q^2_{L5O} = 0.684 …(13)

pIC_{50} (HWB) = 5.318 + 0.583 (0.119) Me + 0.500 (0.215) BELp5 – 1.305 (0.194) JGI7

n = 14, r = 0.918, s = 0.201, F (3, 10) = 17.800, Q^2_{LOO} = 0.742, Q^2_{L5O} = 0.581 …(14)

The F-values for above equations remained significant at 99% level [$F_{2,8}$ (0.01) = 8.649 and $F_{3,10}$ (0.01) = 6.552] while their r-values have accounted, respectively, for 83.9% and 84.3% of variances in the observed activities. The Q^2 (Q^2_{LOO} and Q^2_{L5O}) values are significant enough to divulge substantial internal strength of these models. The participated descriptors, MATS2v and GATS3e, in Equation (13), have highlighted the role of Moran and Geary autocorrelations of lag (path) 2 and lag 3 of the compounds which are weighted, respectively by atomic van der Waals volumes and atomic Sanderson electronegativities. To further improve the activity of compound towards Raw Cells, the value of MATS2v should be higher while the value of GATS3e should be lower. The descriptors, Me, BELp5 and JGI7, appeared in Equation (14), representing, respectively the mean atomic Sanderson electronegativity (scaled on carbon atom), the lowest eigenvalue no. 5 of Burden matrix/ weighted by atomic polarizabilities and the mean topological charge index of order 7. Thus, the electronic and polarization effects appear to dominate during interaction of a compound at receptor sites (HWB). The higher values of descriptors Me and BELp5 and lower value of descriptor JGI7 are advantageous in improving the HWB inhibition activity. The calculated pIC_{50} values, using Equation (13) and (14), are listed in Table 1 for the sake of comparison with the observed ones. The two are found in close agreement with each other.

CONCLUSION

The TACE, MMP-2 and MMP-13 inhibition activity of selective α- and β-sulfone hydroxamates have been quantitatively analyzed in terms of chemometric descriptors. The statistically developed quantitative structure-activity relationship (QSAR) models provided rationales to explain the inhibition activities of these congeners.

For TACE inhibition activity, the descriptors identified through CP-MLR analysis have highlighted the role of the electronic effect and weaker forces (van der Waals and polarization) during interaction with receptor site(s). The flexibility in a compound and presence of certain structural fragment, such as, number of total secondary carbons (sp^3) and number of tertiary amides (aromatic) are prerequisite for inhibition of the MMP-2 while the atom centered fragments (R-C(=X)-X/ R-C#X/ X=C=X) or the number of hydrogen atoms, hydrogen attached to heteroatom and hydrogen attached to C0 (sp^3) with one X attached to next C are responsible for inhibition of the MMP-13. The guidelines included in the discussion may be helpful in exploring more potential analogues of the series. The statistics emerged from the test set have validated the identified significant models. PLS analysis has further confirmed the dominance of the CP-MLR identified descriptors. Applicability domain analysis revealed that the suggested models have acceptable predictability. Except one outlier compound (**A8**; Table 1) for MMP-2 activity, all the compounds were within the applicability domain of the proposed models of TACE, MMP-13 and MMP-2 activities and were evaluated correctly.

The *in vivo* inhibition activities for LPS-stimulated TNF production in Raw Cells and human whole blood (HWB), reported for a few compounds, have also been correlated with chemometric descriptors. The identified descriptors for inhibition of Raw Cells have emphasized the importance of lag 2 and lag 3 of autocorrelations weighted, respectively, by atomic van der Waals volumes and atomic Sanderson electronegativities. Similarly, the electronic and polarizability weighted descriptors have exhibited their worth in the inhibition of HWB.

ACKNOWLEDGEMENT

The financial support provided by the University Grants Commission, New Delhi to one of the author (PS) under the scheme of Emeritus Fellowship is thankfully acknowledged. Authors are also thankful to their Institutions for providing necessary facilities to complete this study.

REFERENCES

1. J. R. Bradley, J. Pathol., **214**, 149 (2008).
2. M. A. Palladino, F. R. Bahjat, E. A. Theodorakis and L. L. Moldawer, Nat. Rev. Drug. Disc., **2**, 736 (2003).
3. R. C. Newton and C. P. Decicco, J. Med. Chem., **42**, 2295 (1999).
4. R. C. Newton, K. A. Solomon, M. B. Covington, C. P. Decicco, P. J. Haley, S. M. Friedman and K. Vaddi, Ann. Rheum. Dis., **60**, 25 (2001).
5. D. Tracey, L. Klareskog, E. H. Sasso, J. G. Salfeld and P. P. Tak, Pharmacol. Ther., **117**, 244 (2008).
6. S. DasGupta, P. R. Murumkar, R. Giridhar and M. R. Yadav, Bioorg. Med. Chem., **17**, 444 (2009).
7. J. S. Skotnicki and J. I. Levin, Ann. Rep. Med. Chem., **38**, 153 (2003).
8. M. L. Moss, L. Sklair-Tavron and R. Nudelman, Nat. Clin. Pract. Rheum., **4**, 300 (2008).
9. R. A. Black, C. T. Rauch, C. J. Kozlosky, J. J. Peschon, J. L. Slack, M. R. Wolfson, B. J. Castner, K. L. Stocking, P. Reddy, S. Srinivasan, N. Melson, N. Bioiani, K. A. Schooley, M. Gerhart, R. Davis, J. N. Fitzner, R. S. Johnson, R. J. Paxton, C. J. March and D. P. Cerretti, Nature, **385**, 729 (1997).
10. M. L. Moss, S. –L. Jin, M. E. Milla, D. M. Bickett, W. Burkhart, H. L. Carter, W. J. Chem, W. C. Clay, J. R. Didsbury, D. Hassler, C. R. Hoffman, T. A. Kost, M. H. Lambert, M. A. Leesnitzer, P. McCauley, F. McGeehan, J. Mitchell, M. Moyer, G. Pahel, W. Rocque, L. K. Overton, R. Schoenen, T. Seaton, J. L. Su, J. D. Becherer et al., Nature, **385** 733 (1997).
11. K. Maskos, C. Fernandez-Catalan, R. Huber, G. P. Bourenkov, H. Bartunik, G. A. Ellestad, P. Reddy, M. F. Wolfson, C. T. Rauch, B. J. Castner, R. Davis, H. R. Clarke, M. Fitzner Petersen, J. N. Fitzner, D. P. Cerretti, C. J. March, R. J. Paxton, R. A. Black and W. Bode, Proc. Natl. Acad. Sci. (USA), **95**, 3408 (1998).
12. M. Whittaker, C. D. Floyd, P. Brown and A. J. H. Gearing, Chem. Rev., **99**, 2735 (1999).
13. K. Park, A. Aplasca, M. T. Du, L. Sun, Y. Zhu, Y. Zhang and J. I. Levin, Bioorg. Med. Chem. Lett., **16**, 3927 (2006).
14. J. C. Condon, D. Joseph-McCarthy, J. I. Levin, H. Lombart, F. E. Lovering, L. Sun, W. Wang, W. Xu and Y. Zhang, Bioorg. Med. Chem. Lett., **17**, 34 (2007).
15. A. M. Venkatesan, J. M. Davis, G. T. Grosu, J. Baker, A. Zask, J. I. Levin, J. Ellingboe, J. S. Skotnicki, J. F. DiJoseph, A. Sung, G. Jin, W. Xu, D. Joseph-McCarthy and D. Barone, J. Med. Chem., **47**, 6255 (2004).
16. C. Zhang, F. Lovering, M. Behnke, A. Zask, V.Sandanayaka, L. Sun, Y. Zhu, W. Xu, Y Zhang and J. I. Levin, Bioorg. Med. Chem. Lett., **19**, 3445 (2009).
17. SYSTAT, Version 7.0; SPSS Inc, 444 North Michigan Avenue, Chicago, IL 60611.
18. ChemDraw Ultra 6.0 and Chem3D Ultra, Cambridge Soft Corporation, Cambridge, USA.
19. DRAGON Software, Version 3.0-2003; by R. Todeschini, V. Consonni, A. Mauri and M. Pavan, Milano, Italy. Available from: http//disat.unimib.it/chm/Dragon.htm.
20. Y. S. Prabhakar, QSAR Comb. Sci., **22**, 583 (2003).
21. A. Golbraikh and A. Tropsha, J. Mol. Graph. Model., **20**, 269 (2002).

22. S. Sharma, B. K. Sharma, S. K. Sharma, P. Singh and Y. S. Prabhakar, Eur. J. Med. Chem., **44**, 1377 (2009).

23. B. K. Sharma, P. Pilania, P. Singh and Y. S. Prabhakar, SAR QSAR Environ. Res., **21**, 169 (2010).

24. B. K. Sharma, P. Singh, K. Sarbhai and Y. S. Prabhakar, SAR QSAR Environ. Res., **21**, 369 (2010).

25. B. K. Sharma, P. Pilania, K. Sarbhai, P. Singh P and Y. S. Prabhakar, Mol. Divers., **14**, 371 (2010).

26. B. K. Sharma, P. Singh, M. Shekhawat, K. Sarbhai and Y. S. Prabhakar, SAR and QSAR in Environ. Res., **22**, 365 (2011).

27. S. –S. So and M. Karplus, J. Med. Chem., **40**, 4347 (1997).

28. Y. S. Prabhakar, V. R. Solomon, R. K. Rawal, M. K. Gupta and S. B. Katti, QSAR Combn. Sci., **23**, 234 (2004).

29. S. Wold, Technomet., **20**, 397 (1978).

30. N. Kettaneh, A. Berglund and S. Wold, Comput. Stat. Data Anal., **48**, 69 (2005).

31. L. Stahle and S. Wold, In: G. P. Ellis, G. B. West, (Eds.), Progress in Medicinal Chemistry, **Vol. 25**, Elsevier Science Publishers, BV (1988) p. 291.

32. P. Gramatica P, QSAR Comb. Sci., **26**, 694 (2007).

33. L. Eriksson, J. Jaworska, A. P. Worth, M. T. D. Cronin, R. M. McDowell and P. Gramatica, Environ. Health Persp., **111**, 1361 (2003).